Exogenous vitamin C boosts the antitumor efficacy of paclitaxel containing reduction-sensitive shell-sheddable micelles *in vivo*

Yaqin Zhu [a,b], Xiuxiu Wang [a], Jian Zhang [a], Fenghua Meng [a], Chao Deng [a], Ru Cheng [a], Jan Feijen [a,b,*], Zhiyuan Zhong [a,**]

[a] Biomedical Polymers Laboratory, and Jiangsu Key Laboratory of Advanced Functional Polymer Design and Application, College of Chemistry, Chemical Engineering and Materials Science, Soochow University, Suzhou 215123, PR China
[b] Department of Polymer Chemistry and Biomaterials, Faculty of Science and Technology, MIRA Institute for Biomedical Technology and Technical Medicine, University of Twente, P.O. Box 217, 7500 AE Enschede, The Netherlands

ABSTRACT

Slow drug release at the tumor tissue and poor tumor penetration are two big challenges for the successful application of nanosystems in tumor therapy. Here, we report that a high concentration of the natural reducing agent vitamin C (VC) triggers rapid extracellular PTX release from PTX-loaded shell-sheddable PEG-SS-PCL micelles (SSM) in tumors *in vivo*. An *in vivo* tolerance study showed that VC at a blood concentration of 40 mM had little toxicity to nude mice. Notably, SSM rapidly disassembled and released the payloads (Cy5 or PTX) in response to 40 mM VC. *In vivo* near-infrared imaging of tumor-bearing mice showed that with post-injection of VC to establish a blood concentration of 40 mM, Cy5 was quickly released from the micelles and diffused deep into the tumor tissue. Biodistribution studies revealed that 6 h after the injection of PTX-loaded micelles the highest tumor accumulation was reached, which was set as the injection time for VC. The antitumor efficacy of a combination therapy of PTX-loaded micelles and VC was evaluated in both MCF-7 and U87MG tumor models. In both tumor models, single injections of VC didn't show any antitumor effect, while sequential administration of PTX-loaded SSM and VC exhibited significantly higher tumor inhibition effects and better survival rates as compared to single treatment with PTX-loaded micelles, demonstrating that exogenous administration of VC effectively triggered the release of PTX from SSM *in vivo*. The combination of reduction-sensitive nanomedicines with exogenous VC appears a promising approach to achieve potent treatment of malignant tumors.

© 2017 Elsevier B.V. All rights reserved.
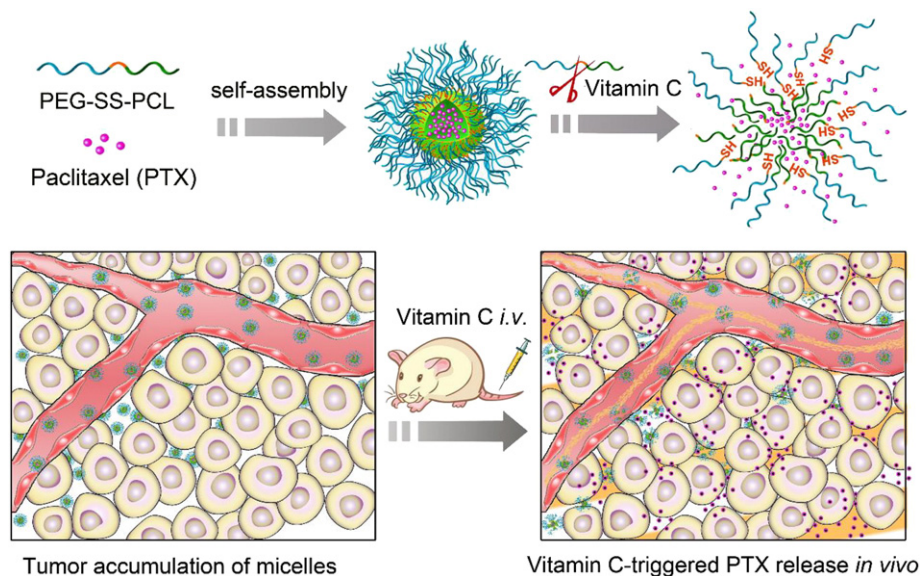
1. Introduction

In recent years, stimuli-responsive nanoparticles have gained considerable attention as they enable rapid drug release at the target site [1–3]. A large body of stimuli-responsive nanoparticles has been designed to become activated inside the tumor cells using the lower pH in early endosomes and lysosomes [4] and higher reducing potential in the cytoplasm [5,6].

In addition to controlled drug release, tumor penetration is another big challenge for anticancer nanomedicines [7,8]. The nanomedicines after arriving at the tumor site cannot penetrate deep into the tumor tissues, because of their large size, high tumor density and interstitial fluid pressure [9,10]. Consequently, most of the nanomedicines are only located at the margin of the tumors where abundant blood vessels exist. This largely limits the antitumor efficacy of nanomedicines that are designed to release drugs inside the tumor cells. In the past years, different efforts have been undertaken to improve the tumor penetration of nanomedicines [11–16]. One of the appealing approaches is to release cytostatic agents in the tumor extracellular space. For example, super pH-sensitive nanosystems were designed to rapidly release drug in response to the slightly acidic pH (pH 6.5–6.8) of the extracellular matrix of the tumor [17–20]. Some nanosystems were developed to respond to enzymes (*e.g.* matrix metalloproteinases, hyaluronidase, furin) in the tumor extracellular matrix [21,22]. Besides the internal stimuli in the tumor microenvironment, external stimuli-sensitive nanosystems have also been studied to achieve accelerated local drug release [23–28]. In this case, dedicated equipment is required and many tumors cannot be easily accessed. Another interesting method is to artificially create or enhance a specific condition by administration of an exogenous agent [29–31]. Lam et al. reported that boronate cross-linked micelles accomplished triggered PTX release and enhanced cytotoxicity to SKOV-3 ovarian cancer cells in the presence of 100 mM mannitol [29]. Kuai et al. reported that post-injection of L-cysteine (a reducing agent)

Scheme 1. Illustration of VC-triggered micelle destabilization and drug release. (A) VC triggers destabilization and PTX release from PTX-loaded SSM by cleaving the interconnecting disulfide bonds; (B) Post-injection of exogenous VC after tumor accumulation of SSM *in vivo* leads to micelle disassembly, rapid extracellular PTX release, and deep tumor penetration.

24 h after administration of liposomes with cell-penetrating TAT peptide shielded by a cleavable long PEG to C26 tumor-bearing mice promoted the uptake of liposomes [30]. *N*-acetylcysteine (NAC) approved by the FDA for mucolytic therapy and for the treatment of acetoaminophen overdose, was used to enhance the reducing level of the tumor tissue and trigger the release of PTX from disulfide cross-linked micelles, leading to improved treatment of SKOV-3 ovarian cancer-bearing mice [31].

In this paper, we report on PTX-loaded redox-sensitive shell-sheddable micelles (SSM) in combination with post-injection of exogenous vitamin C (VC) for triggered rapid release of PTX in the tumor and enhanced drug tumor penetration, resulting in a superior antitumor effect (Scheme 1). It has been reported that VC as a natural antioxidant, is able to reduce disulfide bonds [32,33]. Moreover, compared to other reducing agents like NAC and L-cysteine, VC showed a longer circulating time and has been safely used in clinical trials at a high dose [34,35]. We hypothesized that when shell-sheddable micelles accumulate at the tumor site sufficiently, post-injection of a relatively high dose of VC intravenously will trigger micelle destabilization and rapid local release of PTX, leading to a high therapeutic efficacy. Notably, VC may also be considered as a pro-oxidant which may be toxic to cancer cells [36]. Here, we investigated the effect of exogenous VC on the drug
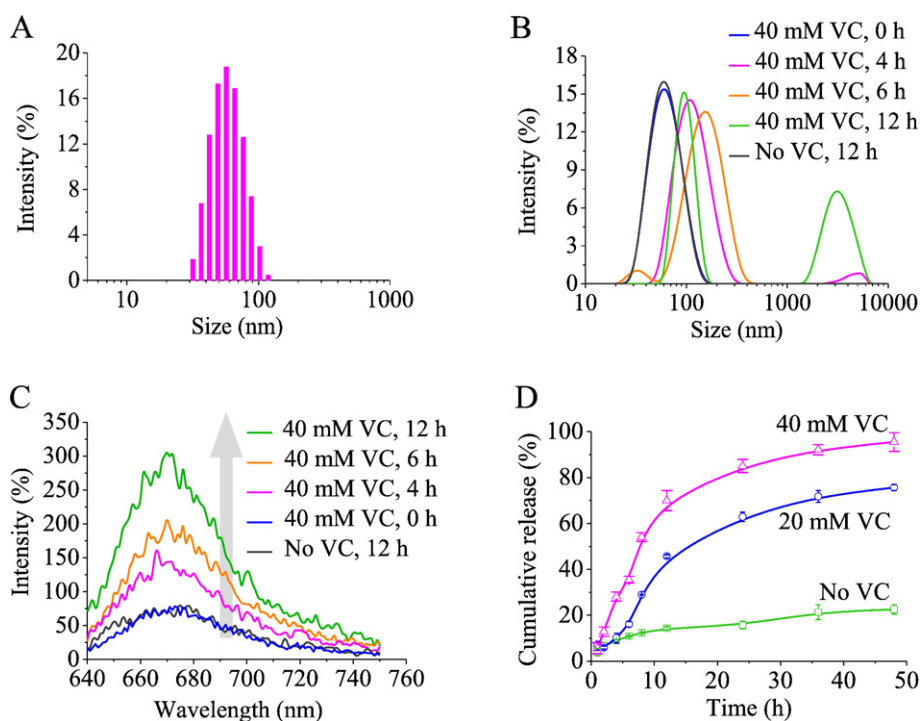

Fig. 1. (A) Size distribution of blank SSM. (B) Size change of SSM in response to 40 mM VC in time (10 mM PB, pH 7.4). (C) Fluorescence excitation spectra of Cy5-loaded SSM in response to 40 mM VC in PB (10 mM, pH 7.4) in time. (D) VC-triggered PTX release from PTX-loaded SSM. Data are presented as mean ± SD (n = 3).

release of PTX-loaded SSM *in vitro* and therapeutic efficacy of PTX-loaded SSM in MCF-7 breast tumor and U87MG glioma models *in vivo*.

2. Materials and methods

2.1. Materials

Poly(ethylene glycol) monomethyl ether (MeO-PEG, M_n = 5.0 kg/mol, Fluka) was dried by azeotropic distillation from anhydrous toluene. Dichloromethane (DCM) was purified using the solvent purification system (Innovative Technology, USA). Sodium ascorbate (VC, 99%, J&K), paclitaxel (PTX, >99%, Beijing Zhongshuo Pharmaceutical Technology Development Co., Ltd., Beijing, China), glutathione (GSH, >98%, Amresco, USA), Cy5 (Mycomebio Biomedical Science and Technology Center, Beijing, China), dibutyltin dilaurate (DBTDL, 97.5%, J&K), N, N-dimethylformamide (DMF, anhydrous, >99.7%, Alfa Aesar), diethyl ether, n-hexane, formaldehyde (Sinopharm Chemical Reagent Co., Ltd., Shanghai, China), methanol, acetonitrile (HPLC grade, Sigma, USA), 2 3-(4,5-dimethylthiazol-2-yl)-2,5-diphenyltetrazolium bromide (MTT, Sigma, USA), trypsin (Jinuo Biomedical Technology, Hangzhou, Zhejiang, China), pentobarbital sodium (Solarbio Science &Technology, Beijing, China), and 96-well plates (Thermo Fisher Scientific, USA) were used as received. Cystamine diisocyanate (CDI) and poly(ε-caprolactone), PCL, M_n (^{1}H NMR) = 2.9 kg/mol, PDI (GPC) = 1.3, were synthesized according to our previous reports [37,38]. Free PTX

(6 mg/mL) was prepared by dissolving PTX in a 1:1 mixture of Cremophor EL and ethanol.

2.2. Cell experiments and animal studies

The human U87MG glioma, MCF-7 breast cancer cells and murine fibroblast L929 cells were purchased from the cell bank of the Chinese Academy of Sciences (Shanghai, China). U87MG and MCF-7 cells were maintained in DMEM medium (HyClone, Logan, Utah, USA) supplemented with 1% penicillin, 1% streptomycin (Jinuo Biomedical Technology, Hangzhou, Zhejiang, China), and 10% fetal bovine serum (FBS, Gibco, Invitrogen, USA). The cells were cultured as a monolayer in a humidified atmosphere containing 5% CO_2 at 37 °C.

Female Balb/c nude mice of 4–6 weeks age (18–22 g) were purchased from the model animal research center of Nanjing University (Nanjing, China). Mice were housed at 25 °C and 55% humidity under natural light/dark conditions and allowed free access to standard food and water. All animal procedures were performed following the protocol approved by the Animal Study Committee of Soochow University (agreement number: 120, date: 12-January-2015).

2.3. VC tolerance in vitro and in vivo

The cytotoxicity of VC to MCF-7, U87 and L929 cells was determined by the MTT assay [39]. Briefly, U87MG, MCF-7 or L929 cells were seeded
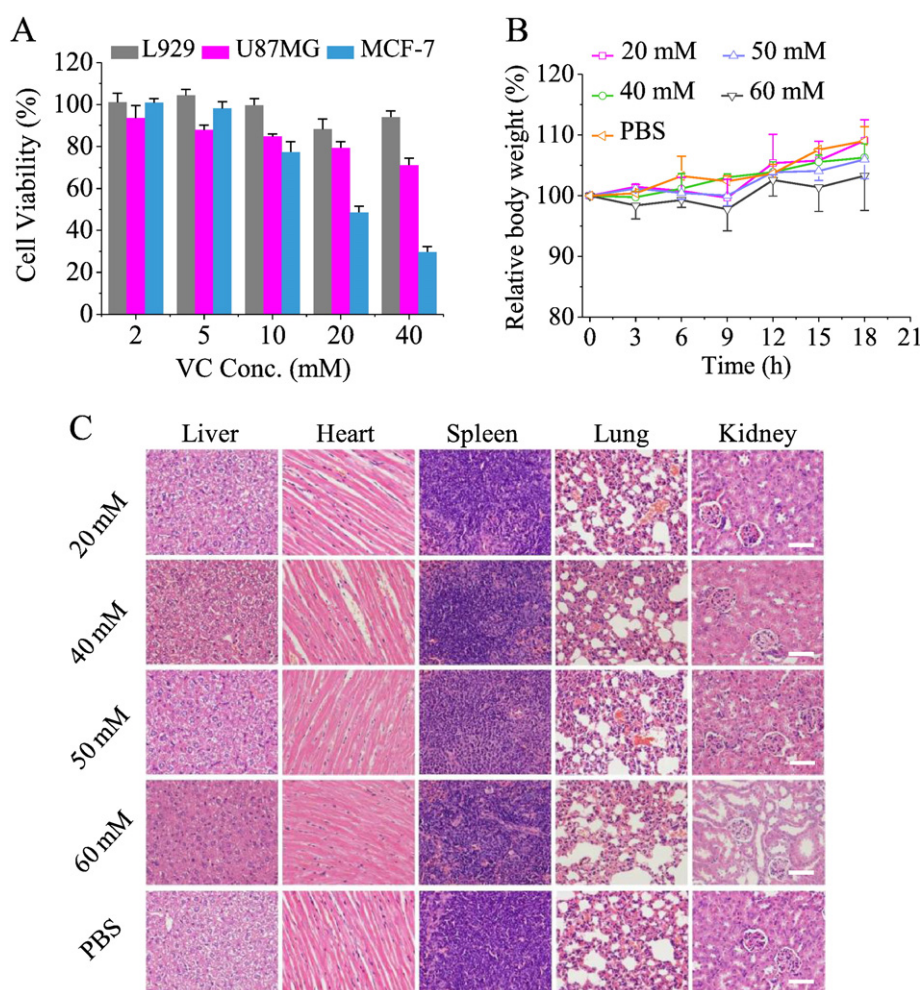

Fig. 2. VC tolerance *in vitro* and *in vivo*. (A) Cytotoxicity of VC against L929 fibroblasts, U87MG glioma cells and MCF-7 breast cancer cells. The cells were incubated with different concentrations of VC for 1 h. After removing the medium, the cells were cultured in fresh medium for another 47 h. Data are presented as mean ± SD (n = 4). (B) Body weight changes of nude mice over a period of 18 days after repeated administration (day 0, 3, 6, 9, 12) of 20, 40, 50 or 60 mM VC (initial blood concentration). Data are presented as means ± SD (n = 5). (C) Histological analysis of liver, heart, spleen, lung and kidney sections excised from Balb/C nude mice at 18 days after VC treatment. The images were obtained by a Leica microscope at 400× magnification. Bar: 50 μm.

at a density of 8×10^3, 5×10^3 cells/well and 5×10^3 cells/well, respectively, in 96-well plates and incubated for 24 h. The prescribed amounts of VC in 10 μL of PBS were added. The cells were incubated for 1 h, the medium was removed and replaced with fresh medium, and the cells were incubated for another 47 h. Subsequently, 20 μL of MTT stock solution (5 mg/mL) was added to each well. The cells were further cultured for 4 h at 37 °C in the dark. The medium was discarded and 150 μL of DMSO was added to dissolve the blue formazan crystals. Cell viability was assessed by the absorbance at 492 nm of the DMSO solution measured on a microplate reader (Multiskan FC, Thermo). The data were expressed as the percentages of viable cells compared to the survival of a control group (untreated cells).

To investigate the VC tolerance *in vivo*, different doses of VC in PB buffer (237 mg/kg, 474 mg/kg, 593 mg/kg and 711 mg/kg), corresponding with an initial VC concentration in blood of 20, 40, 50, and 60 mM, respectively, were injected into nude mice (200 μL per 20 g, 5 mice for each group) on day 0, 3, 6, 9, and 12. The body weight change of the treated mice was monitored until day 18. At the end of the treatment, one mouse of each group was sacrificed, and the main organs including liver, heart, spleen, lung and kidney were excised. The tissues were fixed with 4% formalin solution and embedded in paraffin. The sliced organ tissues (thickness: 4 mm) mounted on glass slides were stained by hematoxylin and eosin (H&E) and observed with a digital microscope (Leica QWin, Germany).

2.4. Preparation of PTX or Cy5-loaded PEG-SS-PCL micelles (SSM)

The synthetic route for PEG-SS-PCL polymer has been shown in Fig. S2. PTX-loaded reduction-sensitive SSM was prepared by directly injecting a mixture of 100 μL of PEG-SS-PCL in DMF (10 mg/mL) and 11 μL of PTX in DMF (10 mg/mL) into 0.9 mL of phosphate buffer (PB, 10 mM, pH 7.4) and standing at room temperature for 2 h to form a homogeneous dispersion, followed by extensive dialysis against PB for 12 h at room temperature. Cy5-loaded SSM was prepared in a similar way except using 4 μL of Cy5 (5 mg/mL in DMF) instead of the PTX solution. DLC and DLE were calculated according to the following formulae:

$$DLC\ (wt\%) = (weight\ of\ loaded\ drug/total\ weight\ of\ polymer\ and\ loaded\ drug) \times 100$$

$$DLE\ (\%) = weight\ of\ loaded\ drug/weight\ of\ drug\ in\ feed \times 100$$

2.5. Serum stability and VC triggered destabilization of SSM

The stability of SSM (1 mg/mL) in the presence of 10% FBS with 20 μM GSH was evaluated by DLS (Malvern Instruments). Briefly, a PEG-SS-PCL micellar dispersion was gently bubbled with nitrogen gas
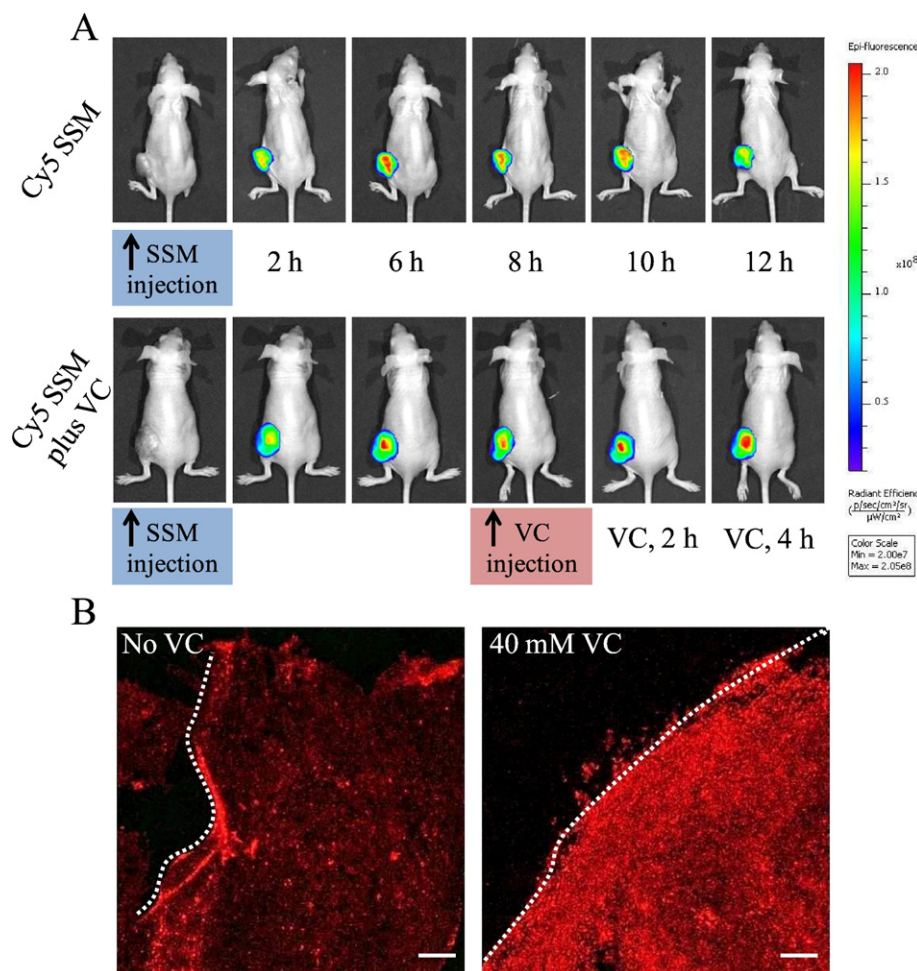
Fig. 3. (A) *In vivo* imaging of Cy5-loaded SSM in MCF-7 tumor bearing mice. VC was injected into group b mice (initial blood concentration 40 mM) 8 h after the injection of Cy5-loaded SSM. (B) Cy5 distribution in MCF-7 tumor tissues observed by confocal microscopy 12 h after injection of Cy5-loaded SSM (left: without VC treatment, right: with VC treatment according to A, group b). Dashed lines indicate the tumor boundary. Bar: 30 μm.
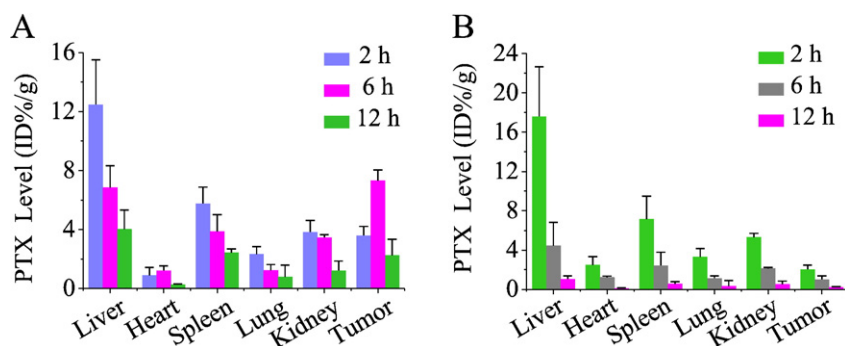
Fig. 4. *In vivo* biodistribution of PTX-loaded SSM (A) and free PTX (B) in MCF-7 tumor-bearing nude mice (5 mg PTX equiv./kg) at 2, 6 and 12 h post injection. Data are presented as mean ± SD ($n = 3$).

for 10 min and a solution of GSH in PB buffer (pH was adjusted to 7.4 with sodium hydroxide) was quickly added (final GSH concentration: 20 μM). Then the sample cuvette was quickly sealed and maintained at 37 °C in a shaking bath (200 rpm). At desired time intervals, the size distributions were determined by DLS.

The destabilization of SSM (1 mg/mL) in response to 20 or 40 mM VC in PB buffer (10 mM, pH 6.8 or 7.4) was investigated by DLS. Briefly, a PEG-SS-PCL micellar dispersion was gently bubbled with nitrogen gas for 10 min, VC was quickly added (final VC concentration: 20 mM or 40 mM) and the dispersion was placed in a shaking bath (200 rpm) at 37 °C in the dark. At different time intervals, the micellar size distribution was measured using DLS.

2.6. VC triggered Cy5 or PTX release

The *in vitro* release of Cy5 from Cy5-loaded micelles in the presence of 40 mM VC in PB buffer was investigated by determination of the

fluorescence of Cy5 released from micelles at different time points. Briefly, Cy5-loaded PEG-SS-PCL micelles (1 mg/mL, Cy5 concentration: 10 μg/mL) was gently bubbled with nitrogen gas for 10 min, VC was quickly added (final VC concentration: 40 mM) and the sample cuvette was quickly sealed and placed in a shaking bath (200 rpm) at 37 °C in the dark. At different time intervals, the Cy5 fluorescence was measured using a fluorescence spectrometer (Thermo Scientific).

The *in vitro* release of PTX from micelles was studied using a dialysis tube (Spectra/Pore, MWCO 12,000) at 37 °C in PB (10 mM, pH 6.8 or 7.4) containing 0.1% (v/v) Tween 80 either in the presence or absence of VC. To acquire sink conditions, drug release studies were performed with 0.5 mL of micelle dispersion (1.0 mg/mL) dialyzing against 25 mL of PB buffer with or without VC (20 or 40 mM). At desired time intervals, 5 mL of release medium was taken out and replenished with an equal volume of fresh medium. The amount of PTX released was determined by HPLC (Shimadzu LC20AD, Japan) with UV detection at 227 nm using a mixture of acetonitrile and water ($v/v = 1/1$) as the mobile
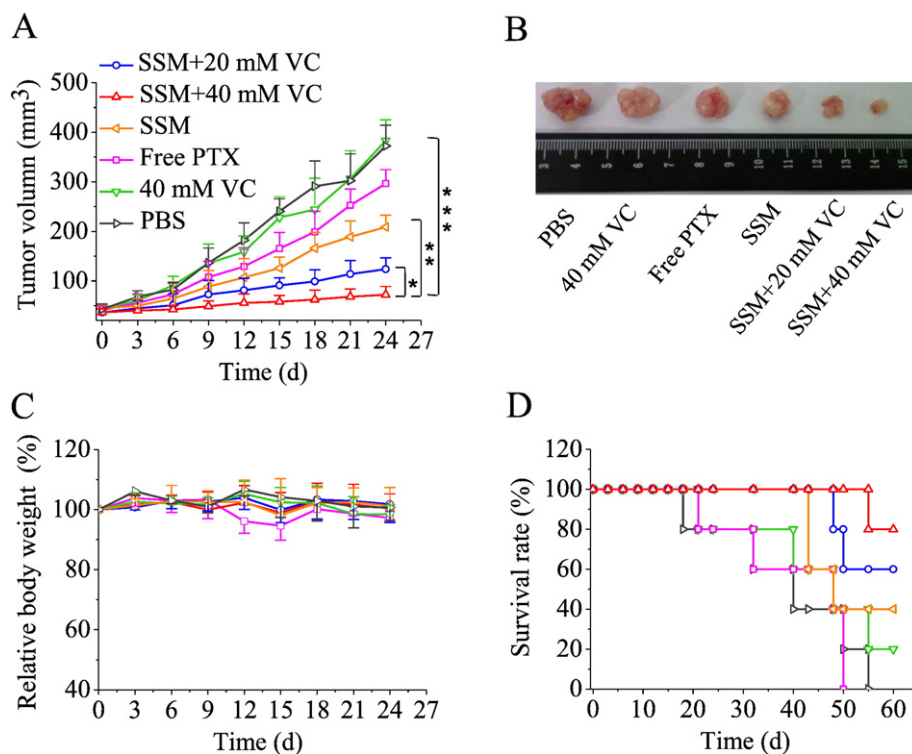

Fig. 5. *In vivo* antitumor efficacy of PTX-loaded SSM with post-injection after 6 h of VC (leading to initial blood concentrations of either 20 or 40 mM VC) in MCF-7 tumor-bearing nude mice. PTX-loaded SSM, free PTX, VC (leading to initial blood concentrations of 40 mM VC) and PBS were used as controls. The drug was given on day 0, 3, 6, 9, 12 (5 mg PTX/kg). (A) Tumor volume changes in time. Data are presented as mean ± SD ($n = 6$). (B) Photographs of tumors collected from different treatment groups on day 24. (C) Body weight changes of nude mice following different treatments within 24 days. (D) Survival rates of mice in different treatment groups within 60 days. Data are presented as means ± SD ($n = 5$). *$p < 0.05$, **$p < 0.01$, ***$p < 0.001$.

phase. Column: Sepax GP-C18 (150 mm × 4.6 mm, 5 μm), flow rate: 1.0 mL/min; injection volume: 20 μL, retention time: 6.3 min.

2.7. In vivo imaging

MCF-7 breast tumor-bearing mice were established as described previously [40]. Briefly, about 1×10^7 MCF-7 cells in 50 μL PBS were subcutaneously injected into the left hind flank of the mice. Tumors were allowed to grow to an average volume of about 100 mm³ in diameter before the experiment. To investigate the tumor accumulation and VC triggered Cy5 release *in vivo*, 200 μL Cy5-loaded SSM were injected in the tumor-bearing mice (3 mice for each group) *via* the tail vein at a Cy5 dose of 250 μg/kg. At 8 h, VC solution (474 mg/kg, 200 μL per 20 g) in PB (10 mM, pH 7.4) leading to an initial VC concentration in blood of 40 mM was injected intravenously to one group of mice, and the other control group was injected with 0.2 mL of PBS (10 mM, pH 7.4). At prescribed time points (2 h, 6 h, 8 h, 10 h, 12 h), the mice were anesthetized with 1% pentobarbital sodium, and whole body fluorescence images were acquired using the Lumina II® imaging system (Caliper Life Sciences) with Ex = 633 nm and Em = 668 nm. After imaging, mice were sacrificed and tumor tissues were taken out and fixed with 4% formalin for 48 h. Then 7 mm sections were cut and studied by confocal laser scanning microscopy (CLSM, Leica TCS SP5, Wetzlar, Germany). The excitation wavelength was set at 633 nm and the emission filter was set at 660 ± 20 nm, and images were obtained using a 63× oil-immersion lens.

2.8. Biodistribution

To quantify the amount of PTX delivered to the tumor and different organs, MCF-7 tumor-bearing mice (3 mice for each group) following 2, 6 and 12 h *i.v.* injection with PTX-loaded SSM or free PTX (5 mg PTX equiv./kg) were sacrificed. The tumor and organs including heart, liver, spleen, lung, and kidney were collected, washed with cold PBS, weighed, and homogenized in 1 mL of methanol. The samples were incubated at −20 °C overnight. After vortexing and centrifugation at 17,226 ×g for 15 min, the supernatant was transferred to a 1.5 mL centrifuge tube and methanol was removed by evaporation. Subsequently, 750 μL of methanol was added and after vortexing and centrifugation at 30,065 ×g rpm for 15 min, the PTX level in the supernatant was determined by HPLC (Shimadzu LC20AD, Japan) with UV detection at 227 nm using a mixture of acetonitrile and water ($v/v = 1/1$) as the mobile phase. Column: Sepax GP-C18 (150 mm × 4.6 mm, 5 μm), flow rate: 1.0 mL/min; injection volume: 20 μL, retention time: 6.3 min. The concentration of PTX was calculated according to a standard curve (Fig. S1).

2.9. In vivo antitumor efficacy

Nude mice bearing MCF-7 breast cancer or U87MG glioma xenografts were used to evaluate the therapeutic efficacy of PTX-loaded SSM with post-injection of either 20 or 40 mM VC. Briefly, about 1×10^7 MCF-7 or U87MG cells in 50 μL PBS were subcutaneously injected into the left hind flank of the mice. The treatments were
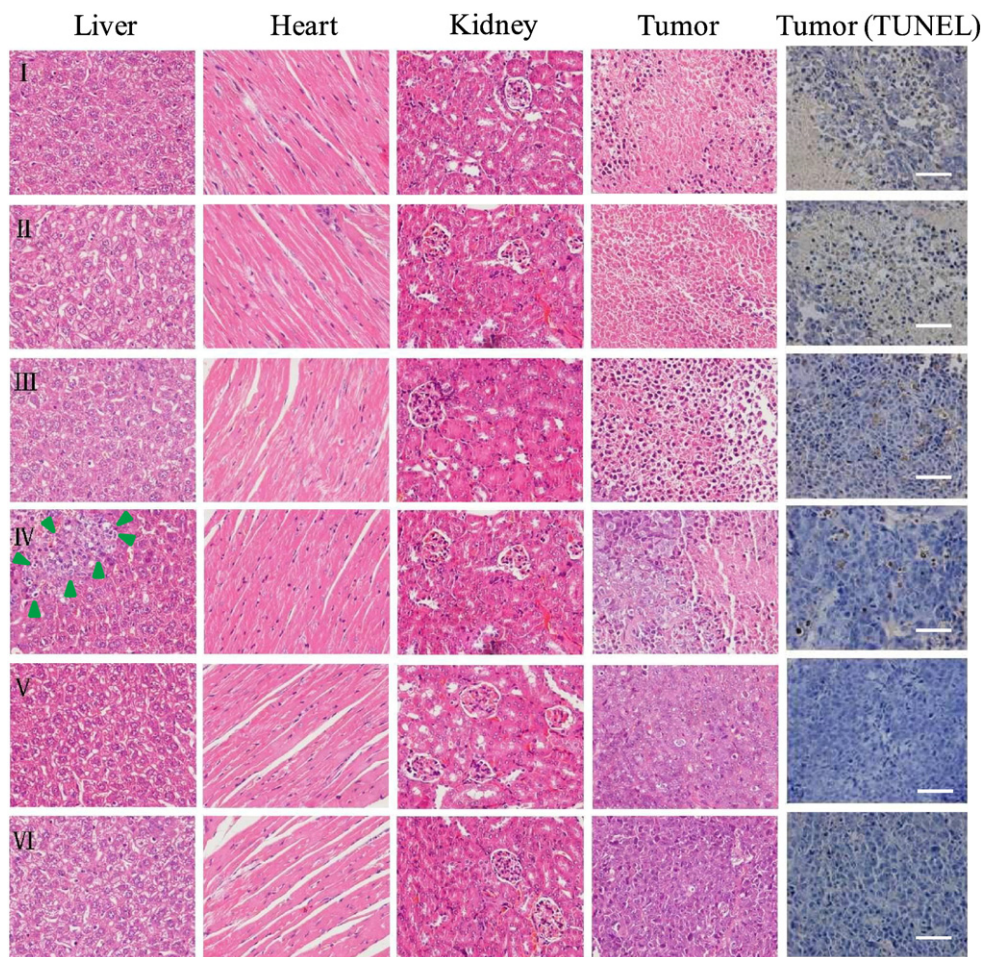
Fig. 6. Sections of liver, heart, kidney and tumor tissue excised from MCF-7 human breast tumor-bearing mice stained by H&E and tumor tissue sections also stained by TUNEL following repeated treatment over a period of 24 days with PTX-loaded SSM with post injections of VC after 6 h (initial blood concentration 20 mM) (I), PTX-loaded SSM with post-injections of VC (initial blood concentration 40 mM) (II), PTX-loaded SSM (III), free PTX (IV), VC (initial blood concentration) 40 mM (V), and PBS (VI). The images were obtained by a Leica microscope at 400× magnification. Green arrows indicate areas of damage in the liver. Bar: 50 μm.

initiated when the tumor reached a volume of 30–40 mm^3. The day starting the treatment was designated as day 0. On day 0, the mice were randomly divided into six groups of 6 mice and injected intravenously *via* the tail vein with the following six formulations, *i.e.* PTX-loaded SSM, PTX-loaded SSM with post-injection at 6 h of VC, leading to initial VC blood concentrations of either 20 or 40 mM, free VC (initial blood concentration of 40 mM), free PTX (PTX dosage: 5 mg/kg) and PBS. The treatment was repeated every 3 days for a total of 5 injections. The tumor sizes were measured by calipers and the volume was calculated according to the formula $V = 0.5 \times L \times W \times H$, wherein L, W and H are the tumor dimensions at the longest, widest and highest direction. Mice in each group were considered to be dead when the tumor volume increased to 1000 mm^3 during treatment. At the end of the treatment, one mouse of each group was sacrificed, and the tumor, liver, heart and kidney were excised. The tissues were fixed with 4% formalin solution and embedded in paraffin. The sliced organ tissues (thickness: 4 mm) mounted on glass slides were stained by hematoxylin and eosin (H&E) and tumor tissues were further stained with terminal deoxynucleotidyl transferase dUTP nick end labeling (TUNEL) and finally observed with a digital microscope (Leica QWin, Germany).

2.10. Statistical analysis

All data are presented as the mean ± standard deviation (SD). One way analysis of variance (ANOVA) with post-hoc tests with the Bonferroni correction was used for comparison between individual groups. *$p < 0.05$, **$p < 0.01$, ***$p < 0.001$.

3. Results and discussion

3.1. VC-triggered drug release from PEG-SS-PCL micelles

Redox-sensitive shell-sheddable micelles have shown significantly enhanced *in vitro* antitumor activity as compared to their reduction-insensitive counterparts, as a result of accelerated drug release inside the tumor cells triggered by intracellular glutathione [38,41–43]. Our recent studies demonstrate that DOX-loaded shell-sheddable PEG-SS-PCL micelles (SSM) exhibit a relatively moderate inhibition of subcutaneous U87MG glioma *in vivo*, likely due to poor tumor cell uptake and tumor penetration [44]. The tumor inhibition of DOX-loaded SSM though improved by installing cRGD ligand remains suboptimal. In this study, we were set to explore means to trigger extracellular, other than intracellular, drug release from SSM in the tumor, which might not only facilitate tumor cell uptake of drug but also greatly enhance drug tumor penetration. It has been reported that drug released in the tumor has a better tumor penetration than the nano-therapeutics [45]. Vitamin C (VC), which plays an important physiological role in cells as a reducing agent and antioxidant, free radical scavenger, and enzyme cofactor [46], was employed to artificially increase the reducing potential in the tumor.

Here, we modified the synthesis of PEG-SS-PCL block copolymer by using cystamine diisocyanate (CDI) as a coupling agent (Fig. S2). ^{1}H NMR (Fig. S3) shows that PEG-SS-PCL had an M_n of 5–2.9 kg/mol. GPC revealed a molecular weight distribution with a moderate M_w/M_n of 1.25 (Fig. S4). PEG-SS-PCL formed small-sized micelles (56 nm, Table S1) as determined by DLS (Fig. 1A). It has been reported that the concentration of GSH in the blood circulation and in extracellular matrices is approximately 2–20 μM [6]. We chose 10% FBS containing 20 μM GSH at pH 7.4 or 6.8 to mimic the *in vivo* blood environment and the slightly acidic tumor extracellular matrix, respectively. As anticipated, SSM was relatively stable under this condition, both at pH 7.4 or 6.8, probably due to the steric protection of the PEG shell [44] (Fig. S5). The size of SSM increased, however, from 60 to 120 nm following 4 h incubation with 40 mM VC (Fig. 1B), indicating that VC effectively triggers rapid disassembly of SSM. A possible mechanism of the cleavage of the disulfide links is the reduction by the abundant reactive ascorbate radicals (AH·) generated by VC [47] (Fig. S6). Apparently the redox potential of the disulfide groups is higher than that of VC [48]. To study whether VC can trigger drug release from SSM, Cy5 and PTX were loaded into SSM. It is known that Cy5 fluorescence is partly self-quenched when Cy5 is loaded into the micellar core due to the homo Förster resonance energy transfer (homo-FRET) effect [49]. Fig. 1C shows that Cy5
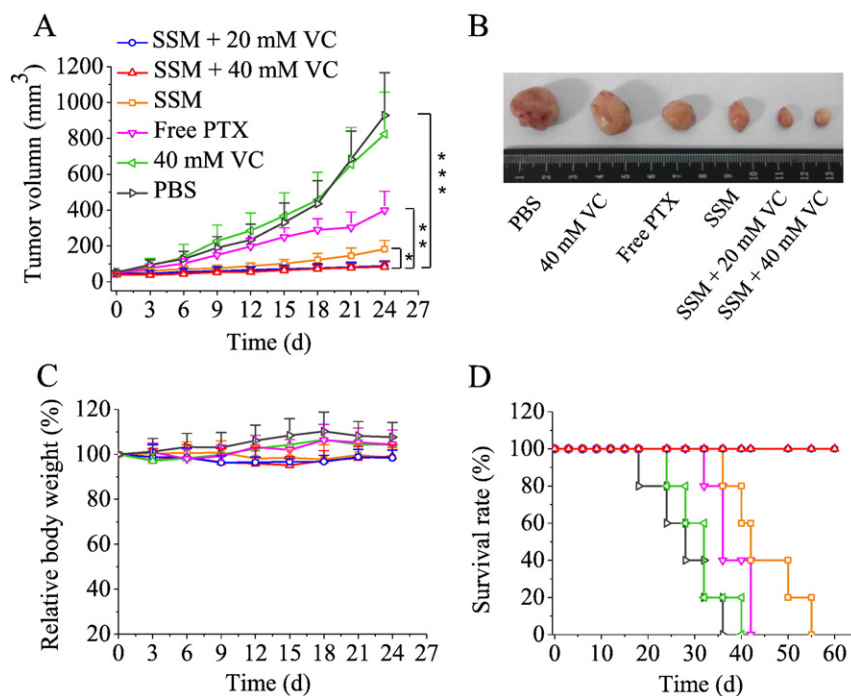
Fig. 7. *In vivo* antitumor efficacy of PTX-loaded SSM with post-injection after 6 h of VC (initial blood concentrations of either 20 or 40 mM) in U87MG tumor-bearing nude mice. PTX-loaded SSM, free PTX, VC (initial blood concentration of 40 mM) and PBS were used as controls. The drug was given on day 0, 3, 6, 9, 12 (5 mg PTX/kg). (A) Tumor volume changes in time. Data are presented as mean ± SD ($n = 6$). (B) Photographs of tumors collected from different treatment groups on day 24. (C) Body weight changes of nude mice following different treatments within 24 days. (D) Survival rates of mice in different treatment groups within 60 days. Data are presented as means ± SD ($n = 5$). *$p < 0.05$, **$p < 0.01$, ***$p < 0.001$.

fluorescence gradually increased with increasing VC incubation time, indicating that release of Cy5 is facilitated by VC. PTX could be easily loaded into SSM with a DLC of 7.8 wt% at a theoretical DLC of 10 wt% (Table S1). Fig. 1D shows that *ca.* 20% PTX was released from SSM in PB (10 mM, pH 7.4) over 48 h. PTX release was significantly accelerated by VC. For example, 62.9% and 85.0% of PTX was released from SSM in 24 h in the presence of 20 and 40 mM VC, respectively. Considering that tumor tissues have a slightly acidic microenvironment, micelle destabilization and PTX release was also investigated at pH 6.8 to evaluate the effect of pH on VC cleavage of disulfide bonds. It was noticed that the size of SSM quickly increased in the presence of VC at pH 6.8 (Fig. S7 A) and the PTX release profile at pH 6.8 (Fig. S7 B) was similar to that at pH 7.4, indicating that VC can effectively cleave disulfide bonds and trigger release of payloads from SSM both at pH 7.4 and at pH 6.8 (pH of the tumor microenvironment).

3.2. VC tolerance in vitro and in vivo

To investigate the cytotoxicity of VC against normal cells and tumor cells, MTT assays were performed with L929 fibroblasts, MCF-7 breast tumor cells and U87MG glioma cells. Fig. 2A showed that VC induced little cytotoxicity to L929 fibroblasts (normal cells) even at a concentration of 40 mM. Notably, VC showed pronounced cytotoxicity to MCF-7 breast cancer cells at concentrations higher than 10 mM. In comparison,

less cytotoxicity was observed in U87MG cells under otherwise the same conditions. It has been reported that different cells have different sensitivities to VC [36]. The high concentrations of VC generate ascorbate radicals and extracellular production of H_2O_2. Variation in VC sensitivity among cancer cells may be related to the complex networks that H_2O_2 acts on combined with the range of functional mutations intrinsic to each cancer cell line [36]. To investigate the *in vivo* tolerance of VC, nude mice were intravenously injected with VC (initial blood concentrations ranging from 20, 40, 50 to 60 mM) on day 0, 3, 6, 9 and 12, respectively. According to the data of a phase II clinical trial, the dose of VC was 1.5 g/kg in patients with cancer. The peak plasma vitamin C concentration was about 32 mM in a patient with body weight of 70 kg (VC was infused at a constant rate over a period of 120 min) [50]. In our study, VC was given to mice by tail-vein injection. In this way the highest blood VC concentration was reached immediately after the VC injection. Therefore we set the highest dose of VC (60 mM) to about twice of that in humans to evaluate the *in vivo* tolerance of VC. Fig. 2B indicates that VC can be well tolerated by mice even at a high VC concentration of 60 mM. H&E staining showed no significant damage of the main organs up to 50 mM VC (Fig. 2C). However, 60 mM VC caused renal edema evidenced by light staining and increased tissue interstitial gaps, probably due to clearance of VC mainly by excretion from the kidneys. Consequently, we chose 40 mM VC as the initial blood concentration for the *in vivo* studies.
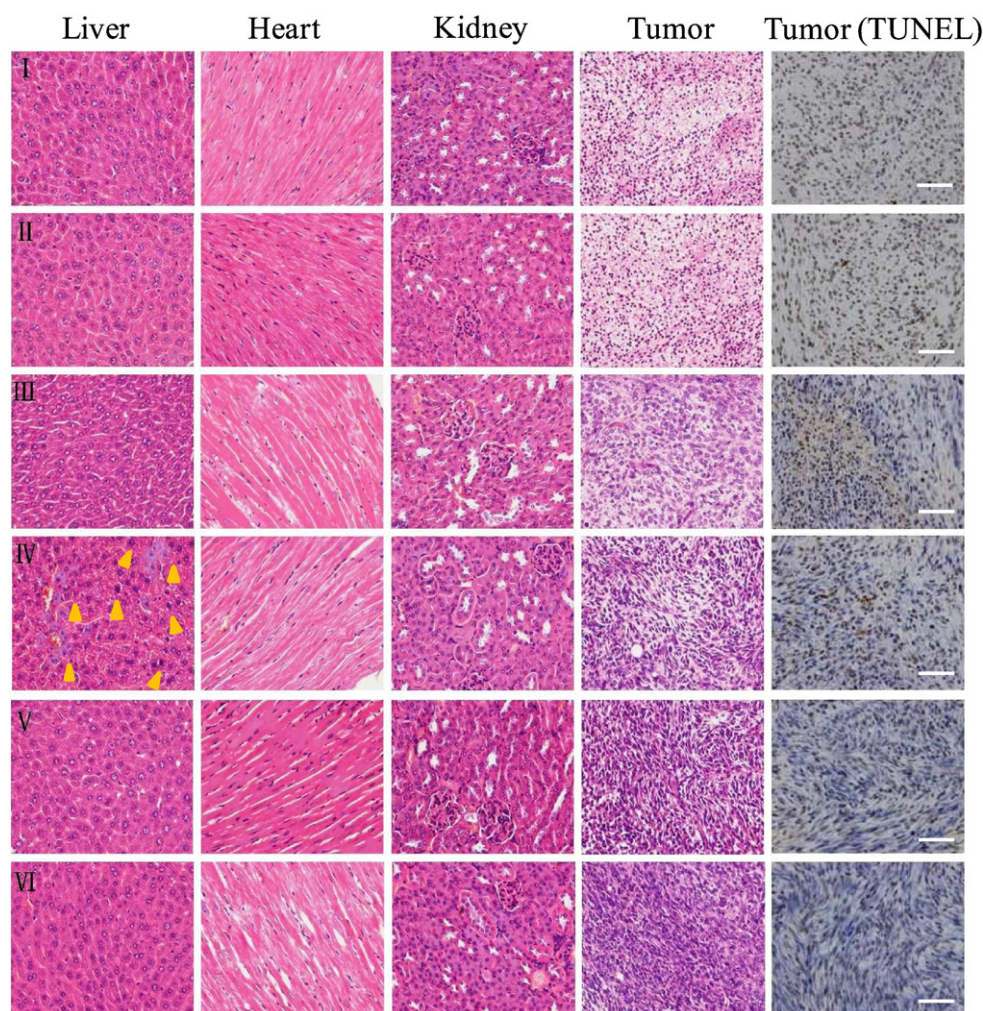
Fig. 8. H&*E*-stained liver, heart, kidney and tumor sections and TUNEL stained tumor slices excised from U87MG tumor-bearing mice following 24 day treatment with PTX-loaded SSM plus 20 mM VC (I), PTX-loaded SSM plus 40 mM VC (II), PTX-loaded SSM (III), free PTX (IV), 40 mM VC (V), and PBS (VI). The images were obtained by a Leica microscope at 400× magnification. Yellow arrows indicate areas of necrosis and apoptosis in the liver. Bar: 50 μm.

3.3. Tumor accumulation and VC-triggered Cy5 release of Cy5-loaded SSM

Cy5-loaded SSM was employed to investigate tumor accumulation and VC-triggered drug release from SSM in MCF-7 tumor bearing mice. Near infrared (NIR) imaging showed that Cy5-loaded SSM accumulated at the tumor site due to the EPR effect (Fig. 3A). Cy5 fluorescence reached a maximum at 6 h. VC was intravenously injected (initial blood concentration of 40 mM) into the mice 8 h after injection of Cy5-loaded SSM. Interestingly, mice treated with VC displayed obviously increased Cy5 fluorescence intensity at the tumor at 4 h post-injection of VC, which was much stronger than for mice without treatment with VC (Fig. 3A). The quantitative analysis (Fig. S8) also showed that the fluorescence intensity at the tumor site of the VC treated group was about 5.4-fold higher than that of the control group at 12 h. The increased Cy5 fluorescence intensity is most likely a result from fast Cy5 release triggered by exogenous VC. It is reported that VC accumulates in solid tumors to concentrations higher than those in the surrounding normal tissue after intravenous administration, probably because VC, as a hexose derivative, was mainly transported into cells in the form of dehydroascorbic acid by glucose transporters (GLUT) [51], which are overexpressed on tumor cells due to their increased glucose metabolism [52]. It has also been reported that after parenteral administration of VC at millimolar levels to rats, ascorbate radical formation took place in the extracellular fluids but not in blood [47]. It is anticipated that the reduction of the disulfide bonds of the polymer used, micellar destabilization and subsequent release of the payload are induced by the concurrent oxidation of VC. We further studied the Cy5 fluorescence in tumor tissue using confocal microscopy. Notably, tumor Cy5 fluorescence in mice without VC treatment was very weak, while strong Cy5 fluorescence throughout the whole tumor tissue was discerned in mice treated with VC (Fig. 3B). As is commonly known tumor penetration of nano-systems is very limited due to their large size and the heterogeneity of tumor tissue [7]. It appears that in our study, i.v. injection of VC can significantly accelerate drug release from SSM in the tumor area and the released drug can then easily penetrate the tumor. A similar phenomenon was also reported by Manzoor et al. who showed that by applying local heat to trigger DOX release from thermally sensitive liposomes at the tumor site, significantly enhanced drug penetration was observed [45].

In our design, VC will be injected at the time when the tumor accumulation of PTX-loaded SSM reaches the highest level. We quantitatively studied the biodistribution of PTX-loaded SSM in MCF-7 tumor-bearing mice at three different time points. The results showed that tumor accumulation of PTX-loaded SSM (Fig. 4A) was significantly higher than that of free PTX (Fig. 4B). Notably, tumor accumulation of PTX-loaded SSM reached 7.3%ID/g at 6 h, which was significantly higher than that at 2 and 12 h. Hence, 6 h post-injection of PTX-loaded SSM seems an optimal time point to inject VC.

3.4. Antitumor efficacy of PTX-loaded SSM enhanced by post-injection of VC

To study the effect of VC on antitumor efficacy of PTX-loaded SSM, we have established MCF-7 breast and U87 glioma subcutaneous tumor models. The PTX-loaded SSM, with or without post-administration of VC (after 6 h) and controls were administered five times over a period of 24 days by intravenous injections according to the scheme of Fig. 5A. Interestingly, post-injection of VC significantly enhanced the tumor inhibitory effect of PTX-loaded SSM in MCF-7 breast tumor-bearing mice (Fig. 5A). Post-injection of VC (initial blood concentration of 40 mM) showed better tumor inhibition than post-injection of VC (initial blood concentration of 20 mM). In contrast, injection of VC (initial blood concentration 40 mM) without pre-administration of PTX-loaded SSM didn't have any antitumor effect, though 40 mM VC exhibited a high cytotoxicity towards MCF-7 cells in vitro. The sensitivity of MCF 7 tumor cells to VC may have been changed in the complex tumor environment in vivo [53]. The photographs of tumors excised on day 24

corroborated that PTX-loaded SSM in combination with 40 mM VC had the smallest tumor size (Fig. 5B). Importantly, both a single VC injection and the combination therapy with PTX-loaded micelles caused no decrease in body weight of nude mice (Fig. 5C), indicating that they have little adverse effects. The survival curves showed that post-injection of VC prolonged the survival time of nude mice (Fig. 5D). H&E staining indicated that PTX-loaded SSM with post-injection of VC had little side effects to the liver, heart and spleen while the free PTX treated group exhibited hepatic damage (Fig. 6, green arrows). It was noted that PTX-loaded SSM in combination with VC resulted in extensive necrosis in the tumor tissues observed from H&E staining. To further study possible apoptosis of the tumor tissue, the TUNEL assay was performed. Images showed that tumor tissue from mice treated with PTX-loaded SSM in combination with 40 mM VC had the highest number of TUNEL positive cells (brown, Fig. 6 II), while that treated with VC alone showed no brown areas, indicating that the apoptosis of tumor tissue was induced by released PTX triggered by VC.

We further verified the effect of VC in U87 glioma subcutaneous tumor-bearing mice, following a similar scheme as for the MCF-7 breast tumor-bearing mice. Notably, the combination of PTX-loaded SSM with either 20 or 40 mM VC showed complete growth inhibition of U87 glioma (Fig. 7A). 40 mM VC alone had no suppression of tumor growth. Fig. 7B confirms that PTX-loaded SSM combined with VC resulted in the smallest tumor size among all treatment groups. Little body weight change was observed for mice treated with PTX-loaded SSM plus VC, PTX-loaded SSM, or 40 mM VC alone (Fig. 7C), further supporting that the combined therapy is well tolerated by mice. Strikingly, all the mice treated with PTX-loaded SSM plus VC, either 20 or 40 mM, survived over an experimental period of 60 days (Fig. 7D). In contrast, mice treated with PTX-loaded SSM and free PTX had short median survival times of 42 and 36 days, respectively. Fig. 8 further corroborates that PTX-loaded SSM plus VC caused little damage to the main organs while significant necrosis (H&E staining) and apoptosis (TUNEL assay, brown nuclei) in the tumor tissue was observed. Free PTX showed toxicity to mice evidenced by some damage in the liver (Fig. 8, yellow arrows). It is clear from the results with both MCF-7 breast and U87 glioma tumor models that 40 mM VC has no tumor inhibition effect while it can significantly improve the antitumor efficacy of PTX-loaded SSM. The enhanced antitumor effect of PTX-loaded SSM plus VC is most likely due to triggered PTX release in the tumor, which facilitates not only tumor cell uptake but also deep tumor penetration. VC is a natural antioxidant and has a high tolerance in mice. Notably, VC possesses several advantages as compared to other reducing agents including NAC. Firstly, vitamin C has a low protein binding rate and circulates mainly in a reduced free form after intravenous injection [54]. In comparison, NAC binds extensively to plasma and tissue proteins after administration due to the high activity of its thiol group, greatly limiting the amount of free circulating NAC [35,55]. The plasma half-life of VC after intravenous injection is about 2 h [34], while that of NAC is 6–40 min [35]. In addition, preclinical studies have shown that high-dose intravenous VC is well tolerated in patients with advanced cancer, indicating its safety in clinical use [34, 50,56]. The combination of reduction-sensitive SSM with VC has appeared as a promising approach to achieve potent treatment of malignant tumors.

4. Conclusion

We have demonstrated that i.v. post-injection after 6 h of exogenous vitamin C to reach an initial blood concentration of 40 mM, significantly boosts the antitumor efficacy of paclitaxel-loaded reduction-responsive shell-sheddable PEG-SS-PCL micelles in subcutaneous human U87MG glioma and MCF-7 breast cancer-bearing nude mice. This enhanced antitumor effect is likely due to fast extracellular PTX release in the tumor triggered by vitamin C, which facilitates not only uptake of PTX by the tumor cells but also deep penetration of PTX in the tumor. Our results show that vitamin C is a new, safe and useful trigger for effective

external activation of reduction-sensitive nanotherapeutics. The combination of reduction-sensitive nanomedicines with administration of exogenous VC appears a promising approach to achieve potent treatment of malignant tumors.

Acknowledgement

Appendix A. Supplementary data

Supplementary data to this article can be found online at http://dx.doi.org/10.1016/j.jconrel.2017.02.002.

References

[1] S. Mura, J. Nicolas, P. Couvreur, Stimuli-responsive nanocarriers for drug delivery, Nat. Mater. 12 (2013) 991–1003.

[2] E. Fleige, M.A. Quadir, R. Haag, Stimuli-responsive polymeric nanocarriers for the controlled transport of active compounds: concepts and applications, Adv. Drug Deliv. Rev. 64 (2012) 866–884.

[3] V.P. Torchilin, Multifunctional, stimuli-sensitive nanoparticulate systems for drug delivery, Nat. Rev. Drug Discov. 13 (2014) 813–827.

[4] K. Zhou, Y. Wang, X. Huang, K. Luby-Phelps, B.D. Sumer, J. Gao, Tunable, ultrasensitive pH-responsive nanoparticles targeting specific endocytic organelles in living cells, Angew. Chem. Int. Ed. 50 (2011) 6109–6114.

[5] R. Cheng, F. Meng, C. Deng, Z. Zhong, Bioresponsive polymeric nanotherapeutics for targeted cancer chemotherapy, Nano Today 10 (2015) 656–670.

[6] F. Meng, W.E. Hennink, Z. Zhong, Reduction-sensitive polymers and bioconjugates for biomedical applications, Biomaterials 30 (2009) 2180–2198.

[7] S. Barua, S. Mitragotri, Challenges associated with penetration of nanoparticles across cell and tissue barriers: a review of current status and future prospects, Nano Today 9 (2014) 223–243.

[8] S. Eetezadi, S.N. Ekdawi, C. Allen, The challenges facing block copolymer micelles for cancer therapy: in vivo barriers and clinical translation, Adv. Drug Deliv. Rev. 91 (2015) 7–22.

[9] P.A. Netti, D.A. Berk, M.A. Swartz, A.J. Grodzinsky, R.K. Jain, Role of extracellular matrix assembly in interstitial transport in solid tumors, Cancer Res. 60 (2000) 2497.

[10] R.K. Jain, T. Stylianopoulos, Delivering nanomedicine to solid tumors, Nat. Rev. Clin. Oncol. 7 (2010) 653–664.

[11] K. Wang, X. Zhang, Y. Liu, C. Liu, B. Jiang, Y. Jiang, Tumor penetrability and anti-angiogenesis using iRGD-mediated delivery of doxorubicin-polymer conjugates, Biomaterials 35 (2014) 8735–8747.

[12] H.J. Li, J.Z. Du, X.J. Du, C.F. Xu, C.Y. Sun, H.X. Wang, Z.T. Cao, X.Z. Yang, Y.H. Zhu, S. Nie, J. Wang, Stimuli-responsive clustered nanoparticles for improved tumor penetration and therapeutic efficacy, Proc. Natl. Acad. Sci. U. S. A. 113 (2016) 4164–4169.

[13] C. Ju, R. Mo, J. Xue, L. Zhang, Z. Zhao, L. Xue, Q. Ping, C. Zhang, Sequential intra-intercellular nanoparticle delivery system for deep tumor penetration, Angew. Chem. Int. Ed. 53 (2014) 6253–6258.

[14] S. Ruan, X. Cao, X. Cun, G. Hu, Y. Zhou, Y. Zhang, L. Lu, Q. He, H. Gao, Matrix metalloproteinase-sensitive size-shrinkable nanoparticles for deep tumor penetration and pH triggered doxorubicin release, Biomaterials 60 (2015) 100–110.

[15] H. Yu, Z. Cui, P. Yu, C. Guo, B. Feng, T. Jiang, S. Wang, Q. Yin, D. Zhong, X. Yang, Z. Zhang, Y. Li, pH- and NIR light-responsive micelles with hyperthermia-triggered tumor penetration and cytoplasm drug release to reverse doxorubicin resistance in breast cancer, Adv. Funct. Mater. 25 (2015) 2489–2500.

[16] J. Li, W. Ke, H. Li, Z. Zha, Y. Han, Z. Ge, Endogenous stimuli-sensitive multistage polymeric micelleplex anticancer drug delivery system for efficient tumor penetration and cellular internalization, Adv. Healthc. Mater. 4 (2015) 2206–2219.

[17] D. Ling, W. Park, S.-j. Park, Y. Lu, K.S. Kim, M.J. Hackett, B.H. Kim, H. Yim, Y.S. Jeon, K. Na, T. Hyeon, Multifunctional tumor pH-sensitive self-assembled nanoparticles for bimodal imaging and treatment of resistant heterogeneous tumors, J. Am. Chem. Soc. 136 (2014) 5647–5655.

[18] Z. Amoozgar, J. Park, Q. Lin, Y. Yeo, Low molecular-weight chitosan as a pH-sensitive stealth coating for tumor-specific drug delivery, Mol. Pharm. 9 (2012) 1262–1270.

[19] K.H. Min, J.-H. Kim, S.M. Bae, H. Shin, M.S. Kim, S. Park, H. Lee, R.-W. Park, I.-S. Kim, K. Kim, I.C. Kwon, S.Y. Jeong, D.S. Lee, Tumoral acidic pH-responsive MPEG-poly(β-amino ester) polymeric micelles for cancer targeting therapy, J. Control. Release 144 (2010) 259–266.

[20] Y. Wang, K. Zhou, G. Huang, C. Hensley, X. Huang, X. Ma, T. Zhao, B.D. Sumer, R.J. DeBerardinis, J. Gao, A nanoparticle-based strategy for the imaging of a broad range of tumours by nonlinear amplification of microenvironment signals, Nat. Mater. 13 (2014) 204–212.

[21] L. Zhu, F. Perche, T. Wang, V.P. Torchilin, Matrix metalloproteinase 2-sensitive multifunctional polymeric micelles for tumor-specific co-delivery of siRNA and hydrophobic drugs, Biomaterials 35 (2014) 4213–4222.

[22] T. Jiang, Z. Zhang, Y. Zhang, H. Lv, J. Zhou, C. Li, L. Hou, Q. Zhang, Dual-functional liposomes based on pH-responsive cell-penetrating peptide and hyaluronic acid for tumor-targeted anticancer drug delivery, Biomaterials 33 (2012) 9246–9258.

[23] J. You, R. Zhang, G. Zhang, M. Zhong, Y. Liu, C.S. Van Pelt, D. Liang, W. Wei, A.K. Sood, C. Li, Photothermal-chemotherapy with doxorubicin-loaded hollow gold nanospheres: a platform for near-infrared light-trigged drug release, J. Control. Release 158 (2012) 319–328.

[24] T. Wang, H. Jiang, L. Wan, Q. Zhao, T. Jiang, B. Wang, S. Wang, Potential application of functional porous TiO$_2$ nanoparticles in light-controlled drug release and targeted drug delivery, Acta Biomater. 13 (2015) 354–363.

[25] J. Ge, E. Neofytou, T.J. Cahill, R.E. Beygui, R.N. Zare, Drug release from electric-field-responsive nanoparticles, ACS Nano 6 (2012) 227–233.

[26] P. Yang, D. Li, S. Jin, J. Ding, J. Guo, W. Shi, C. Wang, Stimuli-responsive biodegradable poly(methacrylic acid) based nanocapsules for ultrasound traced and triggered drug delivery system, Biomaterials 35 (2014) 2079–2088.

[27] H. Oliveira, E. Pérez-Andrés, J. Thevenot, O. Sandre, E. Berra, S. Lecommandoux, Magnetic field triggered drug release from polymersomes for cancer therapeutics, J. Control. Release 169 (2013) 165–170.

[28] H. De Oliveira, J. Thevenot, S. Lecommandoux, Smart polymersomes for therapy and diagnosis: fast progress toward multifunctional biomimetic nanomedicines, Wiley Interdiscip. Rev. Nanomed. Nanobiotechnol. 4 (2012) 525–546.

[29] Y. Li, W. Xiao, K. Xiao, L. Berti, J. Luo, H.P. Tseng, G. Fung, K.S. Lam, Well-defined, reversible boronate crosslinked nanocarriers for targeted drug delivery in response to acidic pH values and cis-diols, Angew. Chem. Int. Ed. 51 (2012) 2864–2869.

[30] R. Kuai, W. Yuan, W. Li, Y. Qin, J. Tang, M. Yuan, L. Fu, R. Ran, Z. Zhang, Q. He, Targeted delivery of cargoes into a murine solid tumor by a cell-penetrating peptide and cleavable poly(ethylene glycol) comodified liposomal delivery system via systemic administration, Mol. Pharm. 8 (2011) 2151–2161.

[31] Y. Li, K. Xiao, J. Luo, W. Xiao, J.S. Lee, A.M. Gonik, J. Kato, T.A. Dong, K.S. Lam, Well-defined, reversible disulfide cross-linked micelles for on-demand paclitaxel delivery, Biomaterials 32 (2011) 6633–6645.

[32] D. Giustarini, I. Dalle-Donne, R. Colombo, A. Milzani, R. Rossi, Is ascorbate able to reduce disulfide bridges? A cautionary note, Nitric Oxide 19 (2008) 252–258.

[33] L.M. Landino, M.T. Koumas, C.E. Mason, J.A. Alston, Ascorbic acid reduction of microtubule protein disulfides and its relevance to protein S-nitrosylation assays, Biochem. Biophys. Res. Commun. 340 (2006) 347–352.

[34] C.M. Stephenson, R.D. Levin, T. Spector, C.G. Lis, Phase I clinical trial to evaluate the safety, tolerability, and pharmacokinetics of high-dose intravenous ascorbic acid in patients with advanced cancer, Cancer Chemother. Pharmacol. 72 (2013) 139–146.

[35] S. Fishbane, N-acetylcysteine in the prevention of radiocontrast-induced nephropathy, J. Am. Soc. Nephrol. 15 (2004) 251–260.

[36] Q. Chen, M.G. Espey, A.Y. Sun, C. Pooput, K.L. Kirk, M.C. Krishna, D.B. Khosh, J. Drisko, M. Levine, Pharmacologic doses of ascorbate act as a prooxidant and decrease growth of aggressive tumor xenografts in mice, Proc. Natl. Acad. Sci. U. S. A. 105 (2008) 11105–11109.

[37] X. Wang, J. Zhang, R. Cheng, F. Meng, C. Deng, Z. Zhong, Facile synthesis of reductively degradable biopolymers using cystamine diisocyanate as a coupling agent, Biomacromolecules 17 (2016) 882–890.

[38] H. Sun, B. Guo, R. Cheng, F. Meng, H. Liu, Z. Zhong, Biodegradable micelles with sheddable poly(ethylene glycol) shells for triggered intracellular release of doxorubicin, Biomaterials 30 (2009) 6358–6366.

[39] Q. Chen, M.G. Espey, M.C. Krishna, J.B. Mitchell, C.P. Corpe, G.R. Buettner, E. Shacter, M. Levine, Pharmacologic ascorbic acid concentrations selectively kill cancer cells: action as a pro-drug to deliver hydrogen peroxide to tissues, Proc. Natl. Acad. Sci. U. S. A. 102 (2005) 13604–13609.

[40] Y. Zhu, X. Wang, J. Chen, J. Zhang, F. Meng, C. Deng, R. Cheng, J. Feijen, Z. Zhong, Bioresponsive and fluorescent hyaluronic acid-iodixanol nanogels for targeted X-ray computed tomography imaging and chemotherapy of breast tumors, J. Control. Release 244 (2016) 229–239.

[41] N.R. Ko, J.K. Oh, Glutathione-triggered disassembly of dual disulfide located degradable nanocarriers of polylactide-based block copolymers for rapid drug release, Biomacromolecules 15 (2014) 3180–3189.

[42] Y. Zhong, W. Yang, H. Sun, R. Cheng, F. Meng, C. Deng, Z. Zhong, Ligand-directed reduction-sensitive shell-sheddable biodegradable micelles actively deliver doxorubicin into the nuclei of target cancer cells, Biomacromolecules 14 (2013) 3723–3730.

[43] C. Shi, X. Guo, Q. Qu, Z. Tang, Y. Wang, S. Zhou, Actively targeted delivery of anticancer drug to tumor cells by redox-responsive star-shaped micelles, Biomaterials 35 (2014) 8711–8722.

[44] Y. Zhu, J. Zhang, F. Meng, C. Deng, R. Cheng, J. Feijen, Z. Zhong, cRGD-functionalized reduction-sensitive shell-sheddable biodegradable micelles mediate enhanced doxorubicin delivery to human glioma xenografts in vivo, J. Control. Release 233 (2016) 29–38.

[45] A.A. Manzoor, L.H. Lindner, C.D. Landon, J.Y. Park, A.J. Simnick, M.R. Dreher, S. Das, G. Hanna, W. Park, A. Chilkoti, G.A. Koning, T.L. ten Hagen, D. Needham, M.W. Dewhirst, Overcoming limitations in nanoparticle drug delivery: triggered, intravascular release to improve drug penetration into tumors, Cancer Res. 72 (2012) 5566–5575.

[46] V. Montecinos, P. Guzman, V. Barra, M. Villagran, C. Munoz-Montesino, K. Sotomayor, E. Escobar, A. Godoy, L. Mardones, P. Sotomayor, C. Guzman, O. Vasquez, V. Gallardo, B. van Zundert, M.R. Bono, S.A. Onate, M. Bustamante, J.G. Carcamo, C.I. Rivas, J.C. Vera, Vitamin C is an essential antioxidant that enhances survival of oxidatively stressed human vascular endothelial cells in the presence of a vast molar excess of glutathione, J. Biol. Chem. 282 (2007) 15506–15515.

[47] J. Du, J.J. Cullen, G.R. Buettner, Ascorbic acid: chemistry, biology and the treatment of cancer, Biochim. Biophys. Acta 1826 (2012) 443–457.

[48] E. Fleming James, G. Bensch Klaus, J. Schreiber, W. Lohmann, Notizen: interaction of ascorbic acid with disulfides, Z. Naturforsch. C 38 (1983) 859.

[49] H. Kobayashi, P.L. Choyke, Target-cancer-cell-specific activatable fluorescence imaging probes: rational design and in vivo applications, Acc. Chem. Res. 44 (2010) 83–90.

[50] L.J. Hoffer, L. Robitaille, R. Zakarian, D. Melnychuk, P. Kavan, J. Agulnik, V. Cohen, D. Small, W.H. Miller, High-dose intravenous vitamin C combined with cytotoxic chemotherapy in patients with advanced cancer: a phase I–II clinical trial, PLoS One 10 (2015) 19.

[51] D.B. Agus, J.C. Vera, D.W. Golde, Stromal cell oxidation: a mechanism by which tumors obtain vitamin C, Cancer Res. 59 (1999) 4555.

[52] L. Szablewski, Expression of glucose transporters in cancers, Biochim. Biophys. Acta 1835 (2013) 164–169.

[53] F. Danhier, O. Feron, V. Préat, To exploit the tumor microenvironment: passive and active tumor targeting of nanocarriers for anti-cancer drug delivery, J. Control. Release 148 (2010) 135–146.

[54] K.R. Dhariwal, W.O. Hartzell, M. Levine, Ascorbic acid and dehydroascorbic acid measurements in human plasma and serum, Am. J. Clin. Nutr. 54 (1991) 712–716.

[55] D. Harada, S. Naito, Y. Kawauchi, K. Ishikawa, O. Koshitani, I. Hiraoka, M. Otagiri, Determination of reduced, protein-unbound, and total concentrations of N-acetyl-L-cysteine and L-cysteine in rat plasma by postcolumn ligand substitution high-performance liquid chromatography, Anal. Biochem. 290 (2001) 251–259.

[56] S. Ohno, Y. Ohno, N. Suzuki, G.-I. Soma, M. Inoue, High-dose vitamin C (ascorbic acid) therapy in the treatment of patients with advanced cancer, Anticancer Res. 29 (2009) 809–815.